buildings

MDPI

Article

Impact of a Switchable Albedo Radiative Cooling Roof on Building Energy Performance

Yiheng Qiao [1,2] and Xinxian Yu [1,*]

[1] School of Automation and Electrical Engineering, Guangdong Polytechnic Normal University, Guangzhou 510665, China
[2] Faculty of Architecture, The University of Hong Kong, Pokfulam Road, Hong Kong SAR, China
* Correspondence: xxyu@gpnu.edu.cn

Abstract

Radiative cooling roofs can reduce cooling demand and achieve subambient surface temperatures under sunlight, but their high solar reflectance can increase heating demand during cold periods. Switchable albedo radiative cooling roofs may mitigate this seasonal trade-off by switching between cooling and heating states. However, their annual building energy effects across different climates remain insufficiently quantified. This study evaluated a mechanically switchable albedo radiative cooling roof using a U.S. Department of Energy strip mall prototype in eight U.S. cities representing distinct climate zones. Four roof configurations were compared: a baseline roof, a traditional cool roof, a non-switchable radiative cooling roof, and a switchable albedo radiative cooling roof. A retrospective monthly state selection procedure was used to combine the results of two fixed-state annual simulations. The modeled coating, based on properties reported in the literature, changed from a solar reflectance of 0.93 under mechanical stretching to 0.05 under mechanical compression while maintaining high thermal emissivity. In climates dominated by cooling demand, the switchable albedo radiative cooling roofs and non-switchable radiative cooling roofs produced similar cooling benefits. In moderate and cold climates, switching avoided annual heating energy penalties while reducing annual cooling electricity use by 12.0–22.8% relative to the baseline. Under the adopted 2018 energy price assumptions, the switchable albedo radiative cooling roof reduced annual cooling and heating expenditure by 1.7–8.4% in moderate and cold climates. The main benefit of switching was therefore the mitigation of seasonal overcooling while retaining radiative cooling benefits in climates with appreciable heating demand.

Keywords: switchable albedo radiative cooling roof; radiative cooling; cool roof; building energy simulation; seasonal overcooling

Check for updates

Academic Editors: Chi Yan Tso and Jianheng Chen

Received: 20 September 2026
Revised: 18 October 2026
Accepted: 21 October 2026
Published: 25 October 2026

Copyright: © 2026 by the authors. Licensee MDPI, Basel, Switzerland. This article is an open access article distributed under the terms and conditions of the Creative Commons Attribution (CC BY) license.

1. Introduction

Buildings account for a considerable share of global energy consumption and greenhouse gas emissions. For residential and commercial buildings in the United States, heat transfer through the building envelope is an important component of space conditioning demand. Previous assessments estimated that roofs account for approximately 12% of heating thermal loads, while heat gains through roofs may contribute approximately 14% of cooling thermal loads, particularly in low-rise buildings [1]. These values are specific to the U.S. building context and vary with building geometry, envelope construction, insulation level, and climate. Therefore, roof technologies that reduce building thermal loads and

energy use are needed. An earlier assessment across 11 U.S. metropolitan areas estimated potential cooling electricity savings from light-colored roofs [2].

Cool roofs have been designed and used as an effective approach for reducing the cooling loads [3–6]. Cool roofs can be implemented using reflective membranes, liquid-applied coatings, coated metal products, and other roofing materials. Their solar reflectance varies with material type and surface finish; for example, white or reflective coatings typically exhibit initial solar reflectance values of approximately 0.60–0.90, while high-reflectance single-ply membranes can reach values above 0.80 [1,7]. The cooling effect is mainly achieved by the white pigments, but they can intrinsically absorb ultraviolet and violet light [8,9]. In recent years, the rapid developments in radiative cooling technology have demonstrated the potential for greater energy saving than that provided by traditional cool roofs. These radiative cooling materials are carefully designed and optimized to yield higher albedo and thermal emissivity. Radiative cooling roofs can achieve subambient surface temperatures by reflecting most incident solar radiation while emitting thermal radiation to outer space through the atmospheric window. For example, the radiative cooling coating reported in Mandal et al. [10] has an albedo of 0.96 and an emissivity of 0.97, exceeding the typical values reported for conventional cool-roof materials. It could achieve a surface temperature 6 K below the ambient air temperature under direct sunlight in the field test [10]. Building energy simulations further indicated that roofs incorporating this radiative cooling coating could approximately double cooling energy savings relative to traditional white roofs [11]. More recently, Jin et al. developed a durable superamphiphobic MgO/SiO_2 radiative cooling coating with a solar reflectance of 95.04% and an emissivity of 96.67% within the atmospheric transparency window. The coating achieved a peak subambient temperature reduction of 7.22 °C under outdoor conditions and exhibited self-cleaning and environmental durability, further improving the practical applicability of radiative cooling coatings for buildings [12]. Radiative cooling materials and their potential building applications have received considerable scientific attention [13], and their building energy and climate benefits have been investigated across different climatic conditions and building types [11,14–30]. For example, the annual cooling electricity consumption of retail buildings in different U.S. cities was estimated to decrease by 12–21% [11]. However, roofs with radiative cooling materials may cause undesirable cooling on cold days, which would lead to a heating energy penalty. The annual penalty in heating energy could increase by 11–46% in the cities reported in Ref. [11]. More recent experimental and numerical evidence has likewise confirmed this seasonal trade-off; Zhang et al. reported that a passive radiative cooling roof reduced the building cooling load by 29.1% but increased the heating load by 4.1% [31]. Seasonal overcooling may offset part of the annual energy-saving benefits of radiative cooling roofs, particularly in climates with substantial heating demand [32].

A roof system that is reflective when buildings need cooling and absorptive when buildings need heating would be an ideal answer to the problem of overcooling [1,33]. Roofs with adjustable solar reflectance are commonly termed switchable albedo radiative cooling roofs. Roof systems with variable reflectance have been investigated as a means of reducing the seasonal limitations of static cool roofs. Previous numerical studies considered roof solar reflectance ranges extending from 0.15 or 0.30 in the low-reflectance state to 0.55–0.85 in the high-reflectance state [34–36]. These studies demonstrated the potential building energy benefits of changing roof reflectance, although a solar reflectance of 0.85 was insufficient to achieve subambient surface cooling under intense direct sunlight [35]. Moreover, the switching approaches prescribed in these studies or triggered by temperature differ from the mechanically reversible coating evaluated here, for which the roof state is selected according to the simulated heating and cooling effects and the corresponding energy costs. In addition to thermochromic switching, adaptive radiative systems based on

mechanical deformation, optical regulation in response to temperature, and electrochromic modulation have also been developed for dynamic thermal management. Among these approaches, mechanical switching was selected in this study because the reported silicone coating provides two clearly defined and reversible solar reflectance states, 0.93 and 0.05, while maintaining nearly constant high thermal emissivity. These properties allow the cooling and heating states to be represented explicitly in the building energy simulations.

Cool-roof research has progressed from conventional high-reflectance roofs and radiative cooling roofs toward adaptive configurations that dynamically regulate solar reflectance and/or thermal emissivity [37]. The switchable silicone coating reported by Zhao et al. [38] uses mechanically induced cavitation to create two reversible optical states (Figure 1). Under tensile deformation, cavities form within the silicone layer and scatter incident solar radiation, producing a high-reflectance cooling state with a solar reflectance of 0.93. Mechanical compression closes these cavities and restores optical transmission to the underlying solar-absorbing layer, producing a low-reflectance heating state with a solar reflectance of 0.05. The thermal emissivity remains approximately 0.94 in both states.

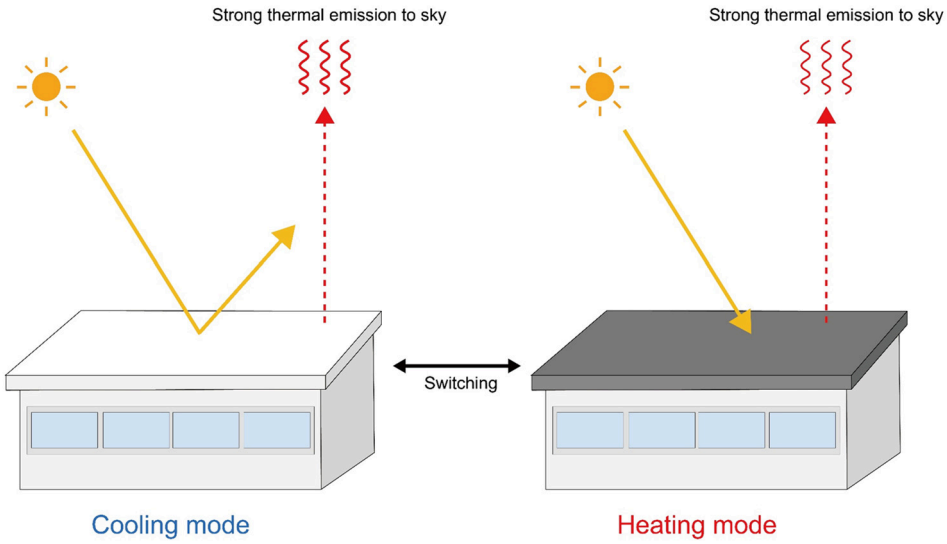


Figure 1. Schematic of the cooling and heating operating states of the switchable albedo radiative cooling roof.

Beyond mechanically switchable solar reflectance, radiative materials that respond to temperature, electrochromic materials, and other adaptive systems have subsequently been developed to dynamically regulate radiative cooling and heating according to environmental conditions [39–41]. Tang et al. developed a radiative roof coating whose thermal emissivity adapts automatically to temperature [40], while Sui et al. demonstrated electrochromic modulation of thermal emissivity for building thermal regulation throughout the year [41]. More recently, adaptive solar and radiative thermoregulators have further extended dynamic regulation toward building thermal management responsive to multiple stimuli [39]. At the building scale, dynamic integration of radiative cooling and solar heating has also been shown to improve annual energy performance, although the resulting benefit depends strongly on climate, building thermal demand, and the operating strategy [42,43]. These studies indicate that switchable albedo radiative cooling roofs should be evaluated not only in terms of optical properties of the material but also through their interaction with building heating and cooling loads.

To address this research gap, this study evaluates a mechanically switchable albedo radiative cooling roof applied to a U.S. Department of Energy strip mall prototype. EnergyPlus simulations were conducted for eight U.S. cities representing distinct climate

zones. Four roof configurations were compared: the baseline roof, a traditional cool roof, a non-switchable radiative cooling roof, and a mechanically switchable albedo radiative cooling roof. A retrospective monthly operating state selection framework was applied to determine the cooling or heating state according to the simulated heating and cooling effects and the corresponding energy costs. The analysis quantifies annual cooling electricity use, heating natural gas use, and energy expenditure to determine whether switching can mitigate seasonal overcooling without sacrificing the cooling benefit of radiative roofs and to identify the climatic conditions under which switching provides the greatest annual energy and expenditure benefits.

2. Methodology

The methodological framework is summarized in Figure 2. DOE strip mall prototype models for each location and TMY3 weather files were used to develop the baseline and alternative roof cases. The radiative cooling calculation was evaluated against previously reported experimental data, after which annual EnergyPlus simulations with fixed properties were conducted for each roof state and city. Monthly cooling electricity and natural gas for heating outputs were aggregated across the ten thermal zones and used for monthly operating state selection. The selected monthly results were then aggregated to evaluate annual cooling and heating energy use and the corresponding energy cost.

2.1. Mechanically Switchable Albedo Radiative Material

The mechanically switchable silicone coating reported in Ref. [38] was selected as the representative adaptive radiative cooling material in this study. Its optical state can be reversibly controlled through mechanical deformation. When mechanical stimuli are applied, cavitation develops from metastable surface creases and generates a porous structure that strongly scatters solar radiation. In this state, the solar reflectance reaches approximately 0.93, while the high longwave emissivity enables radiative heat rejection and subambient cooling.

Mechanical compression restores the coating to a transparent state, allowing sunlight to reach the underlying carbon-black-loaded PDMS layer and enabling approximately 95% solar absorption by the bilayer [38]. The material can be implemented either as a freestanding film or as a coating integrated with a roof surface, with stretching and compression used to switch between the two states. Experimental measurements reported in Ref. [38] showed a daytime surface temperature approximately 5 °C below ambient under hot conditions, whereas in the heating state the surface temperature increased from approximately 10 to 28 °C under cold conditions. These characteristics make the material suitable for investigating the energy implications at the building scale of dynamically switching between solar-reflective cooling and solar-absorptive heating states.

2.2. Archetype Buildings and Building Energy Model

The DOE commercial prototype strip mall model developed for ANSI/ASHRAE/IES Standard 90.1-2019 was adopted as the baseline building model [44,45]. The prototype models were developed by Pacific Northwest National Laboratory in support of the U.S. Department of Energy Building Energy Codes Program and represent multiple commercial building types and climate locations [45]. Among the available commercial prototypes, the strip mall was selected because its low-rise form and relatively large roof area exposed to outdoor conditions make its heating and cooling loads particularly responsive to changes in roof solar reflectance and thermal emissivity. Figure 3 shows the strip mall prototype used in this study, and its principal building and system parameters are summarized in Table 1. The Building Energy Codes Program also provides access to the prototype models [45].

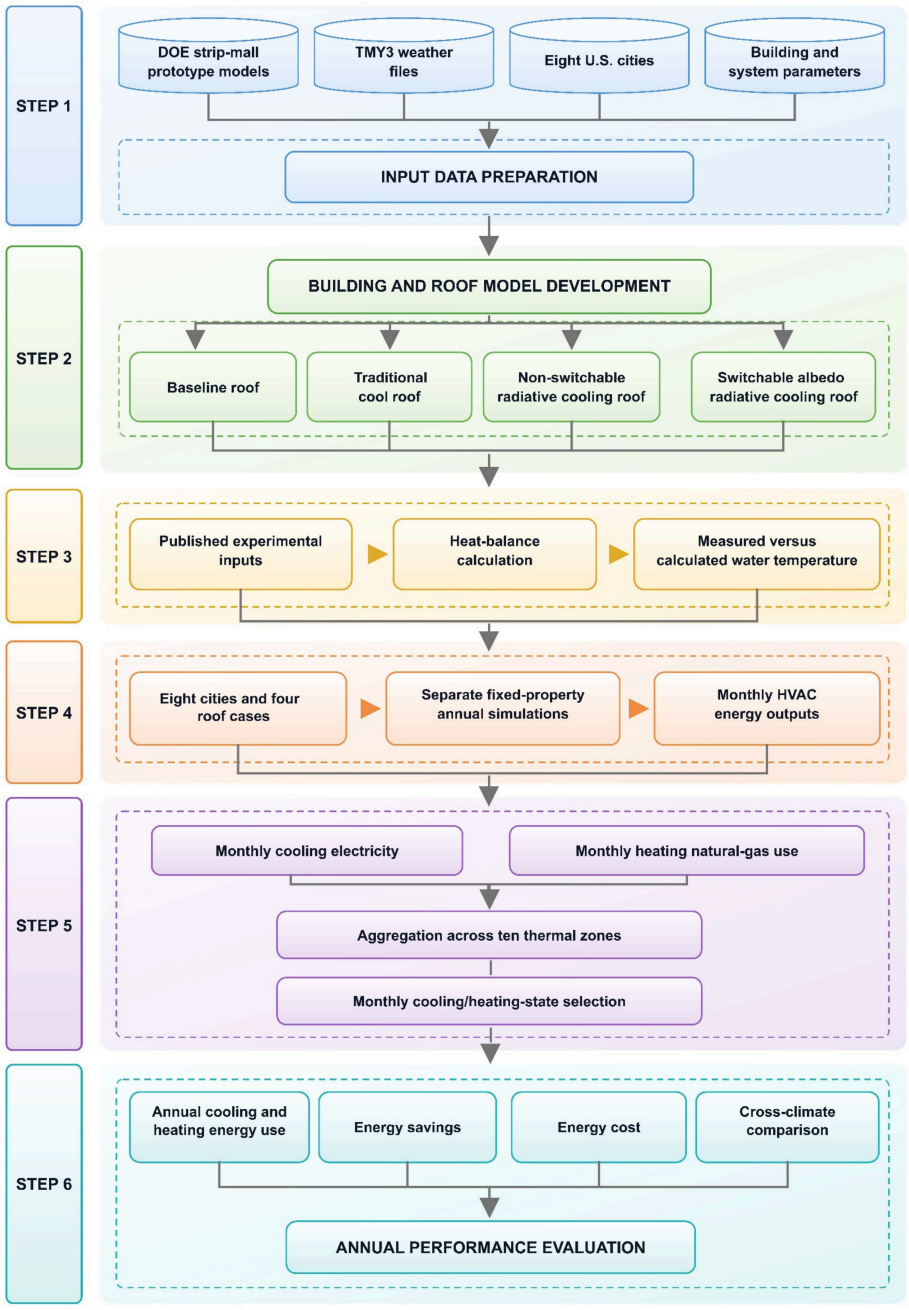


Figure 2. Methodological framework used to evaluate the mechanically switchable albedo radiative cooling roof across eight U.S. cities. The workflow comprises input data preparation, building and roof model development, validation of the radiative cooling calculation, annual EnergyPlus simulations with fixed properties, monthly output processing and operating state selection, and annual energy and cost evaluation.

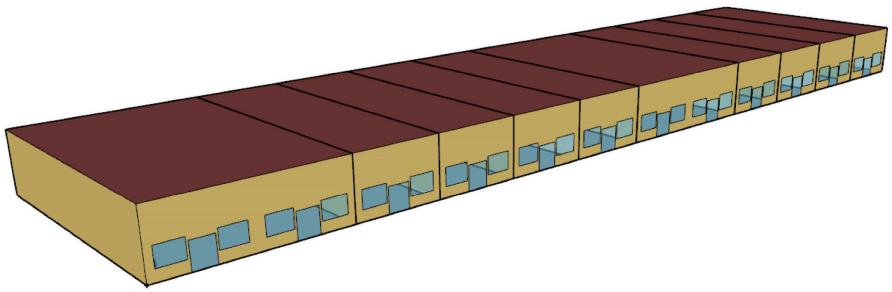


Figure 3. Schematic of the strip mall archetype building used in this study.

Table 1. Principal characteristics of the DOE strip mall prototype models for the selected climates used in this study [44].

Item	Details
Building type	Retail
Building prototype	Strip mall
Building area	2090.32 m^2
HVAC thermostat setpoint	Cooling: 23.9 °C, Heating: 21.1 °C
HVAC thermostat setback	Cooling: 29.4 °C, Heating: 15.6 °C
Unit area ventilation rate	1.2 L/(s·m^2)
Occupants	11.6 m^2/person
Lighting	17.65 W/m^2 (area-weighted average)
Plug and process	4.31 W/m^2
Window-to-wall ratio	10.5%
Roof R-value	3.53 m^2·K/W (Honolulu)
	4.38 m^2·K/W (Tucson, San Diego)
	5.37 m^2·K/W (New York, Denver, Rochester)
	6.15 m^2·K/W (International Falls, Fairbanks)
Wall R-value	1.27 m^2·K/W (Honolulu)
	1.94 m^2·K/W (Tucson)
	2.13 m^2·K/W (San Diego)
	2.60 m^2·K/W (New York)
	3.05 m^2·K/W (Denver)
	3.44 m^2·K/W (Rochester, International Falls)
	4.61 m^2·K/W (Fairbanks)
Glazing representation	Equivalent performance glazing system modeled using the EnergyPlus WindowMaterial:SimpleGlazingSystem object; individual pane, gap, and coating layers were not explicitly resolved.
Window system properties [a]	Honolulu: 2.84 W/(m^2·K)/0.23/0.25 Tucson: 2.56 W/(m^2·K)/0.25/0.28 San Diego: 2.38 W/(m^2·K)/0.25/0.28 New York: 2.044 W/(m^2·K)/0.36/0.396 Denver: 2.04 W/(m^2·K)/0.38/0.42 Rochester: 1.93 W/(m^2·K)/0.38/0.42 International Falls: 1.65 W/(m^2·K)/0.40/0.44 Fairbanks: 1.48 W/(m^2·K)/0.40/0.44
Longwave emissivity	Not independently specified [b]

[a] Window system properties are reported in the order of U-factor, solar heat gain coefficient (SHGC), and visible transmittance. SHGC and visible transmittance are dimensionless. [b] Longwave emissivity was not specified independently because it is not a direct input parameter of the EnergyPlus WindowMaterial:SimpleGlazingSystem object. EnergyPlus generates an equivalent glazing layer from the specified U-factor, SHGC, and visible transmittance.

Annual whole-building simulations were performed using EnergyPlus version 9.0.1, which has been applied in previous studies at the building scale of cool roofs and radiative cooling systems [11,24,25,28,46,47]. The strip mall model comprises ten thermal zones with

a total modeled floor area of 2090.32 m^2. Six timesteps per hour were used, corresponding to a 10-min zone timestep. Heat conduction through opaque envelope components was calculated using the Conduction Transfer Function method, the TARP algorithm was applied to both interior and exterior surface convection, and solar distribution was treated using the FullInteriorAndExterior option. Each of the ten thermal zones was served by a packaged single-zone air-conditioning system. The system comprised an air-cooled two-speed direct-expansion cooling coil, a natural gas heating coil, and a two-speed supply fan with discrete speed control. Cooling and heating capacities and supply-air flow rates were autosized using the EnergyPlus design-day calculations. The natural gas heating coil had a burner efficiency of 0.81, and the outdoor-air controller used differential-enthalpy economizer control. The thermostat setpoints and setback temperatures are reported in Table 1. Except for the roof construction and the corresponding optical properties, the building geometry, internal-load schedules, thermostat settings, and HVAC configuration were kept identical among the roof cases.

This study evaluated whether applying a switchable albedo radiative coating to the roof could avoid the seasonal overcooling associated with a non-switchable radiative cooling roof while improving annual energy performance. EnergyPlus, which has been widely used to investigate building-integrated radiative cooling [11,24,25,28,46,47], was used for the simulations. A layer representing the switchable albedo radiative material was added above the conventional roof assembly of the strip mall prototype. The surface energy balance for this exterior material layer was expressed as follows:

$$q_{sol} + q_{LWR} + q_{conv} - q_{con} = 0 \quad (1)$$

where q_{sol} is the absorbed solar radiation heat flux, q_{LWR} is the longwave radiation, q_{conv} is the convection with the ambient air, and q_{con} is the conduction to the wall. The absorbed solar radiation can be calculated by [48]:

$$q_{sol} = (1 - \mathrm{A}) \cdot I_{sol} \quad (2)$$

where A is the albedo of the material, and I_{sol} is the incident solar radiation. The longwave radiation can be calculated by [48]:

$$q_{LWR} = \varepsilon\sigma F_{gnd}\left(T_{gnd}^4 - T_{mat}^4\right) + \varepsilon\sigma F_{sky}\left(T_{sky}^4 - T_{mat}^4\right) + \varepsilon\sigma F_{air}\left(T_{air}^4 - T_{mat}^4\right) \quad (3)$$

where ε is the constant longwave emissivity of the material; σ is the Stefan–Boltzmann constant; F_{gnd}, F_{sky}, and F_{air} are the view factors of the material surface to the ground, sky, and air, respectively; and T_{gnd}, T_{mat}, T_{sky}, and T_{air} are the ground surface, material surface, sky, and air temperatures, respectively. The view factors can be calculated by [48]:

$$F_{gnd} = 0.5(1 - cos\ \phi) \quad (4)$$

$$F_{sky} = 0.5(1 + cos\ \phi)\sqrt{0.5(1 + cos\ \phi)} \quad (5)$$

$$F_{air} = 0.5(1 + cos\ \phi)\left(1 - \sqrt{0.5(1 + cos\ \phi)}\right) \quad (6)$$

where ϕ is the tilt angle of the material surface. EnergyPlus calculates the sky temperature, T_{sky}, by [48]:

$$T_{sky} = \left(\left(0.787 + 0.764 \cdot \ln\left(\frac{T_{dp}}{273.15}\right)\right) \cdot \left(1 + 0.0224N - 0.0035N^2 + 0.00028N^3\right) \cdot {T_{air}}^4\right)^{0.25} \quad (7)$$

where T_{dp} (K) is the outdoor dewpoint temperature, and N is the opaque sky cover ($N = 0$ when the sky is clear).

A constant longwave emissivity was adopted in the EnergyPlus simulations rather than explicitly resolving the spectral emissivity of the coating. This approximation is appropriate because the selected material [38] exhibits a high and relatively uniform emissivity over the longwave spectral range and can therefore be treated as a broadband emitter. To examine the effect of this simplification, Figure 4 compares the spectral irradiance obtained using a constant emissivity of 0.94 with that calculated from the measured spectral emissivity reported in Ref. [38]. The integrated irradiance differed by only 0.03%. Previous studies at the building scale have also shown that, for broadband radiative cooling materials, the use of a representation with constant emissivity produces little difference in predicted building energy demand relative to a spectral model [11,49]. Accordingly, a constant emissivity of 0.94 was used for the switchable silicone coating in the present simulations.

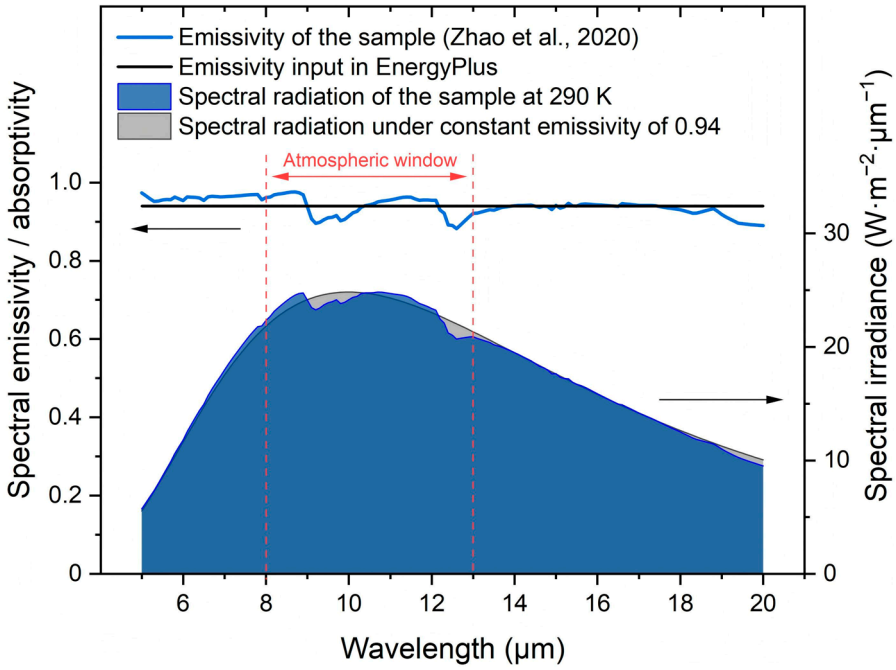


Figure 4. Comparison of the spectral irradiance calculated from the constant emissivity used in this study and the spectral emissivity [38].

2.3. Selected Cities and Weather Data

Hourly Typical Meteorological Year 3 (TMY3) weather data from the National Renewable Energy Laboratory dataset were supplied to EnergyPlus in EnergyPlus Weather (EPW) format [50]. Each EPW file contained 8760 hourly records representing one non-leap typical meteorological year. The NREL TMY3 dataset was developed using meteorological records from 1976–2005 or 1991–2005, depending on data availability at individual weather stations. Because a TMY3 file is assembled from representative months selected from different historical years, it does not represent observations from a single consecutive calendar year. The simulations therefore characterize typical historical weather conditions rather than a specific actual year.

The principal meteorological variables used in the building and roof heat-balance calculations included outdoor dry-bulb temperature, dew-point temperature, relative humidity, atmospheric pressure, direct normal and diffuse horizontal solar radiation, wind speed and direction, and total and opaque sky cover. These variables determine the exterior convective heat transfer, incident solar radiation, sky temperature, and longwave radiative

exchange at the roof surface. Eight cities were selected to represent ASHRAE climate zones 1A–8, covering very-hot humid, hot-dry, warm-marine, mixed-humid, cool-dry, cold-humid, very-cold, and subarctic/arctic conditions. This selection enables the performance of the switchable albedo radiative cooling roof to be evaluated across climates dominated by cooling demand, mixed climates, and climates dominated by heating demand. The same weather file was applied to all roof cases within each city to ensure a consistent comparison. The representative weather stations and their World Meteorological Organization (WMO) identifiers are listed in Table 2.

Table 2. Selected U.S. cities and corresponding ASHRAE thermal climate zones.

City	Climate Zone Number	Climate Classification	TMY3 Weather Station and WMO ID
Honolulu, HI	1A	Very hot humid	Honolulu International Airport, 911820
Tucson, AZ	2B	Hot dry	Tucson–Davis Monthan AFB, 722745
San Diego, CA	3C	Warm marine	San Diego–Brown Field Municipal Airport, 722904
New York, NY	4A	Mixed humid	John F. Kennedy International Airport, 744860
Denver, CO	5B	Cool dry	Denver–Aurora–Buckley AFB, 724695
Rochester, MN	6A	Cold humid	Rochester International Airport, 726440
International Falls, MN	7	Very cold	International Falls International Airport, 727470
Fairbanks, AK	8	Subarctic/Arctic	Fairbanks International Airport, 702610

All weather files were obtained from the NREL TMY3 dataset in EPW format and contained 8760 hourly records.

2.4. Roof Properties

Table 3 summarizes the solar reflectance and thermal emissivity of the four roof configurations. The mechanically switchable silicone coating reported in Ref. [38] was used to define the switchable albedo radiative cooling roof. Its high-reflectance cooling state was also modeled as the non-switchable radiative cooling roof. For comparison, a traditional cool roof with a solar reflectance of 0.70 and a thermal emissivity of 0.90 was defined according to previous studies [11,14]. The baseline case retained the original roof properties of the EnergyPlus strip mall prototype [44].

Table 3. Solar reflectance, thermal emissivity, and data sources for the switchable albedo radiative cooling roof, non-switchable radiative cooling roof, traditional cool roof, and baseline roofs for each city used in the EnergyPlus simulations.

Roof	Albedo	Emissivity	Reference
Switchable albedo radiative cooling roof	0.93/0.05	0.94	Zhao et al. [38]
Non-switchable radiative cooling roof	0.93	0.94	Zhao et al. [38]
Traditional cool roof	0.70	0.90	Baniassadi et al. [11]
Baseline (Honolulu, Tucson, and San Diego)	0.55	0.75	ANSI/ASHRAE/IES Standard 90.1-2019 [44]
Baseline (New York, Denver, Rochester, International Falls, and Fairbanks)	0.23	0.90	ANSI/ASHRAE/IES Standard 90.1-2019 [44]

For each city, the corresponding DOE prototype model was used as the baseline case [44,45]. The alternative roof cases were created by modifying only the exterior layer of the non-residential roof construction, while the remaining envelope components, building geometry, internal loads, schedules, thermostat settings, and HVAC systems were held constant. The traditional cool roof was assigned a solar reflectance of 0.70 and a thermal emissivity of 0.90 [11,14]. The fixed radiative cooling state was assigned a solar reflectance

of 0.93 and a thermal emissivity of 0.94, whereas the solar-absorbing heating state was assigned a solar reflectance of 0.05 and the same thermal emissivity of 0.94 [38]. These optical properties were treated as spatially uniform and time-invariant throughout the simulations. Partial or nonuniform actuation, cyclic degradation, soiling, weather exposure, maintenance downtime, and snow coverage were not represented. In EnergyPlus, solar absorptance was specified as 1-A, where A is the solar reflectance, and thermal absorptance was set equal to the adopted longwave emissivity. Accordingly, the cooling- and heating state input files used solar absorptances of 0.07 and 0.95, respectively, for the exterior roof material, corresponding to solar reflectances of 0.93 and 0.05. All other model inputs were unchanged between the two state simulations.

The optical properties were held constant during each individual EnergyPlus simulation. The cooling and heating states were therefore simulated separately, and the annual performance of the switchable albedo radiative cooling roof was subsequently constructed by selecting one of the two fixed-state results for each month. Transition time, transient optical states, and mechanical actuation energy were not represented in the EnergyPlus model.

2.5. Retrospective Monthly Operating State Selection

EnergyPlus reported monthly cooling-coil electric energy and heating-coil natural gas energy for each of the ten thermal zones. The values for each zone were summed to obtain the monthly whole-building cooling electricity use and heating natural gas use. EnergyPlus outputs in joules were converted to megajoules before the energy cost calculation. Hourly facility electricity and natural gas meters were additionally retained for quality checking and for the analysis of representative days.

Monthly operating state selection was based on the results of the two fixed-state simulations described above. Building type, thermal mass, climate, insulation level, and occupancy schedule can affect the preferred roof state [1]. For each month, cooling electricity savings and heating natural gas penalties were first evaluated for the fixed cooling state relative to the baseline roof. The cooling state was selected when cooling savings occurred without a heating penalty, whereas the heating state was selected when a heating penalty occurred without cooling savings. When cooling savings and heating penalties occurred within the same month, the combined monthly cooling and heating expenditure was calculated for both states using the electricity and natural gas prices reported by the U.S. Energy Information Administration [51] and listed in Table 4. The state with the lower combined monthly expenditure was selected.

Table 4. State-level average retail electricity prices and commercial natural gas prices used in the analysis for the selected cities in 2018 [51].

City	Commercial Natural Gas Price ($/MJ)	Average Retail Electricity Price ($/MJ)
Honolulu, HI	0.0293	0.0811
Tucson, AZ	0.0082	0.0301
San Diego, CA	0.0081	0.0461
New York, NY	0.0070	0.0412
Denver, CO	0.0065	0.0278
Rochester, MN	0.0067	0.0288
International Falls, MN	0.0067	0.0288
Fairbanks, AK	0.0095	0.0538

The monthly operating sequence was constructed retrospectively by post-processing the outputs of the two fixed-state simulations. The selected state was assumed to remain active throughout the corresponding calendar month. When two consecutive months were assigned different states, the change was assumed to occur instantaneously at the boundary between the months. No transition period or transient optical state was represented in the EnergyPlus model. Mechanical actuation energy was also excluded because the experiment at the material scale did not provide a validated actuator at the roof scale model or a quantitative estimate of the energy required for switching.

All expenditure calculations used the 2018 commercial electricity and natural gas prices listed in Table 4. These prices were treated as fixed coefficients throughout the annual calculation. Seasonal tariff variations, demand charges, inflation, and subsequent energy price escalation were not considered. The resulting expenditure estimates therefore represent a scenario based on the adopted 2018 prices rather than current or forecast economic performance.

The annual energy and expenditure values were estimated by selecting and combining monthly outputs from two annual simulations with fixed roof properties. This retrospective procedure was used to assess the potential benefits of monthly state selection. It does not represent a continuous simulation of roof state changes or a directly implementable control rule.

2.6. Validation of the Radiative Cooling Heat Transfer Calculation

The validation focused specifically on the radiative cooling heat transfer calculation used in the roof surface energy balance. The calculation was evaluated against the outdoor water cooling experiment conducted in Boulder, Colorado, USA, on 28 February 2018, and reported by Zhao et al. [52]. The experimental water temperature trajectory between 09:00 and 16:00 was used as the reference [52].

The time-varying ambient air temperature, wind speed, solar irradiance, and cloud cover fraction reported for the experiment were prescribed as boundary inputs. The initial water temperature was −1.87 °C. The seven-hour validation period comprised 281 records at 90-s intervals. The longwave emissivity and solar absorptance of the radiative cooling surface were set to 0.86 and 0.035, respectively. The exterior convective heat transfer coefficient was calculated as $h = 8.3 + 2.5v$, where v is the wind speed in m s^{-1}.

At each time step, the longwave radiative exchange with the sky and surroundings, convective heat transfer with the ambient air, and absorbed solar radiation were calculated. The water temperature was then updated according to the transient energy balance:

$$q_{con} = \frac{c_p m}{A_r} \frac{\partial T_w}{\partial t} \tag{8}$$

where c_p is the effective specific heat capacity of the water container system, m is its total mass, A_r is the radiative surface area exposed to the sky, and T_w is the water temperature. The calculated water temperature trajectory was compared with the experimental measurements, as shown in Figure 5. To quantify the agreement, the mean absolute error (MAE), root-mean-square error (RMSE), mean bias error (MBE), and residual-based coefficient of determination (R^2) were calculated over the 281 paired records. The resulting MAE, RMSE, MBE, and R^2 were 0.658 °C, 0.755 °C, +0.637 °C, and 0.906, respectively, and the maximum absolute error was 1.511 °C. Because MBE was defined as the calculated temperature minus the measured temperature, its positive value indicates a modest warm bias and a slight underestimation of the radiative cooling magnitude. The agreement supports the use of the adopted radiative cooling heat transfer calculation in the subsequent roof simulations. The scope of this comparison is limited to the surface heat transfer calculation under the

prescribed experimental boundary conditions; it does not constitute an independent validation of the complete EnergyPlus strip mall model or the retrospective monthly operating state selection procedure.

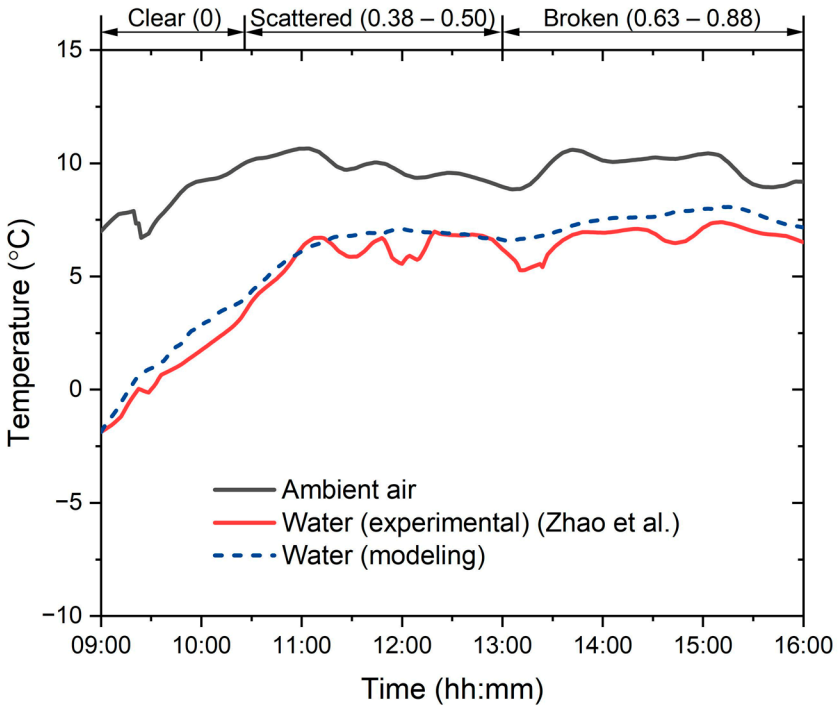


Figure 5. Comparison between the calculated and experimentally measured water temperatures for the outdoor experiment conducted on 28 February 2018, as reported by Zhao et al. [52].

3. Results

3.1. Energy Performance of the Switchable Albedo Radiative Cooling Roof in New York

With the building energy simulation model, this study calculated the hourly energy consumption for cooling and heating in strip malls with different roofs listed in Table 3 in the eight U.S. cities throughout the year. Taking the strip mall in New York as an example, Figures 6a and 6b show the calculated results on 21 July (a typical summer day) and 21 January (a typical winter day), respectively. On 21 July, the switchable albedo radiative cooling roof was in the cooling state, which decreased the exterior roof surface temperature significantly, from 67.2 °C to 29.4 °C, at 12:00 PM compared with the baseline roof. The exterior surface temperature of the switchable albedo radiative cooling roof remained below the ambient dry-bulb temperature for most of the day. Consequently, the use of the switchable albedo radiative cooling roof reduced the cooling electricity use for the strip mall by 9.3% on that day. As a comparison, the traditional cool roof only reduced the cooling electricity use by 5.8% on that day, which was less than the roof with radiative cooling materials. Furthermore, the traditional cool roof could not achieve subambient temperature in the daytime. On 21 January, the switchable albedo radiative cooling roof was in the heating state in accordance with the control strategy. In New York, a strip mall requires heating in winter. The calculated results show that the exterior surface temperature of the switchable albedo radiative cooling roof was slightly higher than the ambient temperature during the daytime. Consequently, not only was overcooling avoided, but the heating energy consumption was reduced slightly, by 0.9%, compared with the baseline roof.

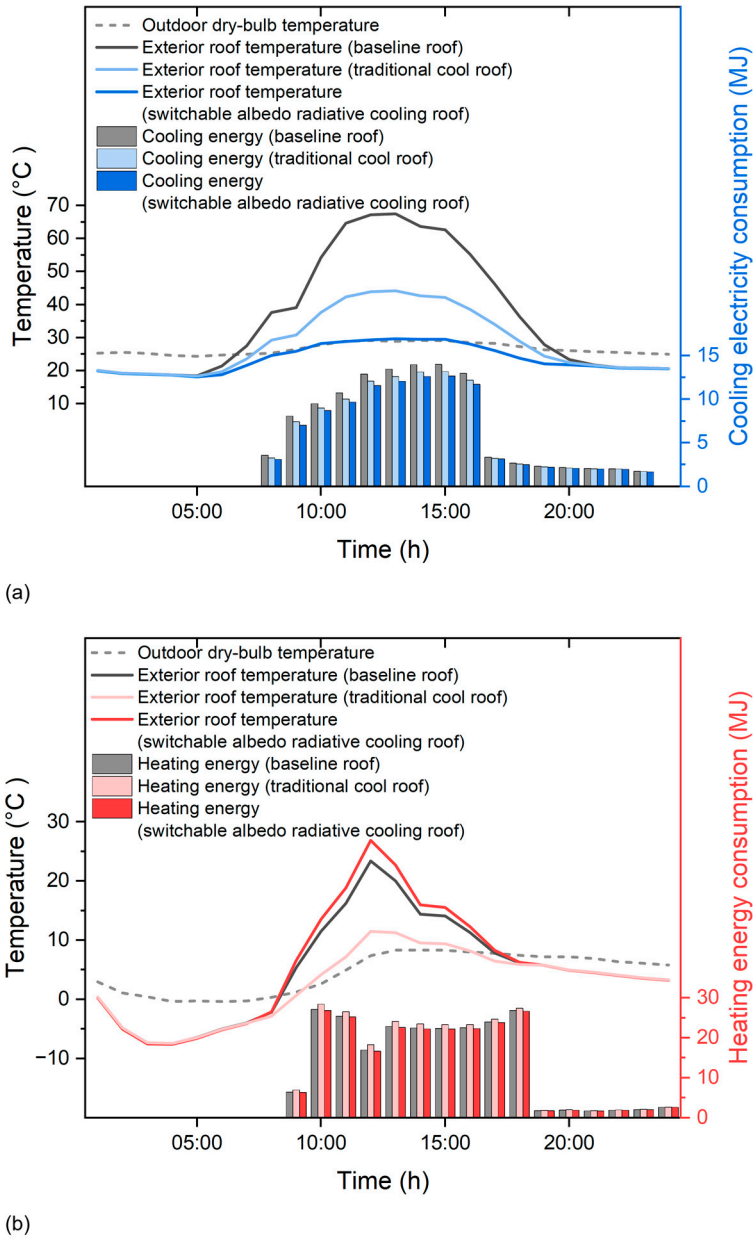


Figure 6. Calculated exterior roof surface temperature and energy consumption in the strip mall with different roofs in New York on (**a**) 21 July (a typical summer day) and (**b**) 21 January (a typical winter day).

3.2. Switchable Albedo Radiative Cooling Roof in Different Cities

With the calculated hourly energy consumption, the monthly cooling electricity and heating natural gas consumption in the strip malls with and without the switchable albedo radiative cooling roof were calculated for the eight U.S. cities. This study grouped the eight cities into three categories according to climate. The hot climate category included Honolulu, Tucson, and San Diego. As shown in Figure 7, the switchable albedo radiative cooling roof was in the cooling state throughout the year in Honolulu. The monthly cooling electricity saving ranged from 5.5% to 9.5%. In Tucson, the heating state was selected only for February, in accordance with the control strategy used in this study. From April to October, the monthly cooling electricity saving ranged from 5.3% to 12%. In San Diego, although heating was required on some days between December and March, using the cooling state for the switchable albedo radiative cooling roof provided a greater monthly dollar cost saving than using the heating state.

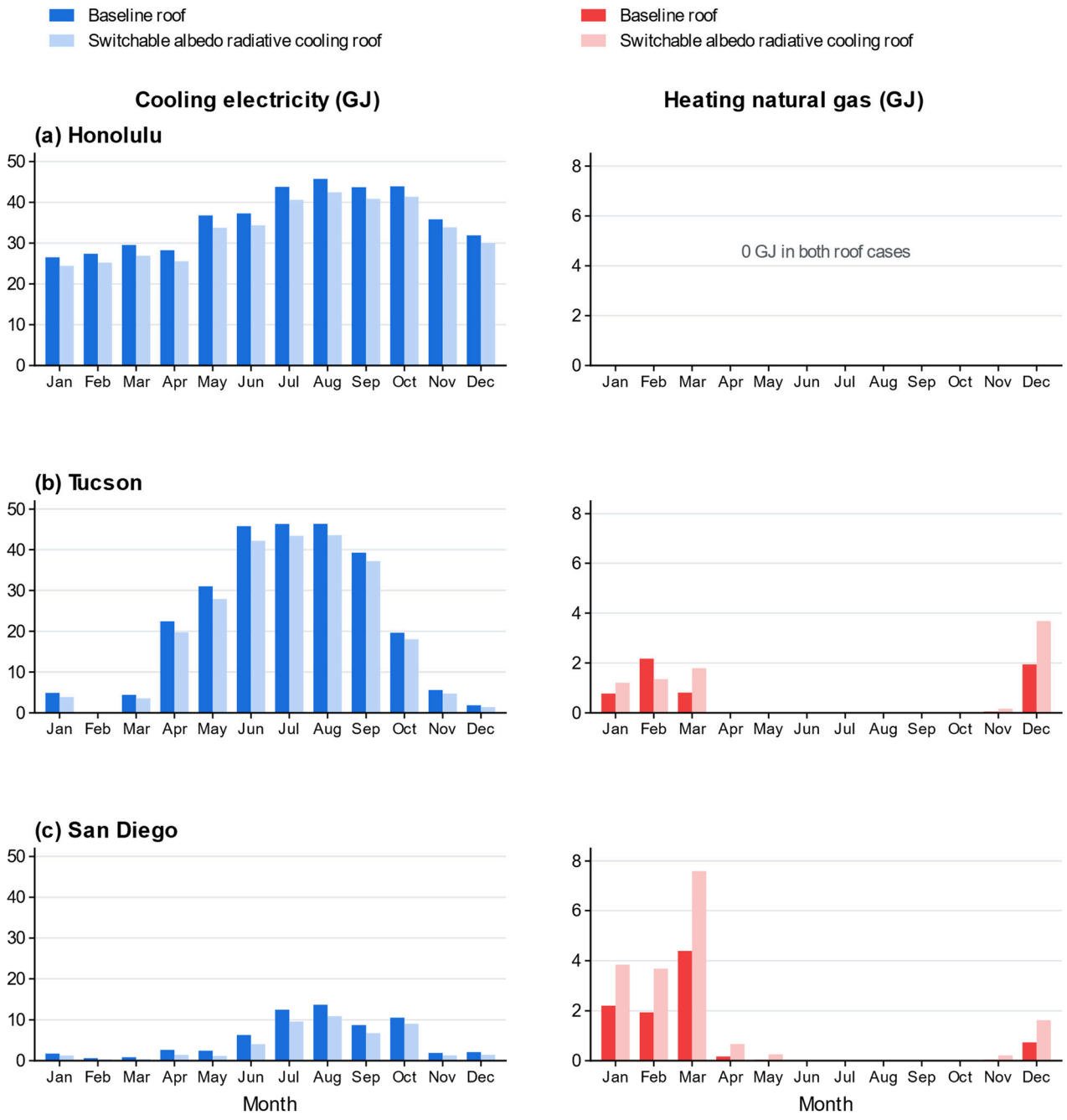


Figure 7. Calculated monthly energy consumption in strip malls with and without the switchable albedo radiative cooling roof in cities in hot climates: (**a**) Honolulu, (**b**) Tucson, and (**c**) San Diego.

New York and Denver were categorized into the moderate climate, with a hot summer and cold winter. As shown in Figure 8, for the switchable albedo radiative cooling roof, the cooling state was selected during the hot seasons, while the heating state was selected during the cold seasons. In New York, the reduction in the monthly cooling electricity use ranged from 9.3% to 15.3% with the use of the switchable albedo radiative cooling roof from June to September. Furthermore, overcooling was avoided, and the reduction in the monthly heating natural gas consumption ranged from 0.9% to 4.6% during the period from November to April. In Denver, the heating state was selected from October to April. Relative to the baseline roof, the selected heating state reduced monthly heating natural gas use by up to 4.6%.

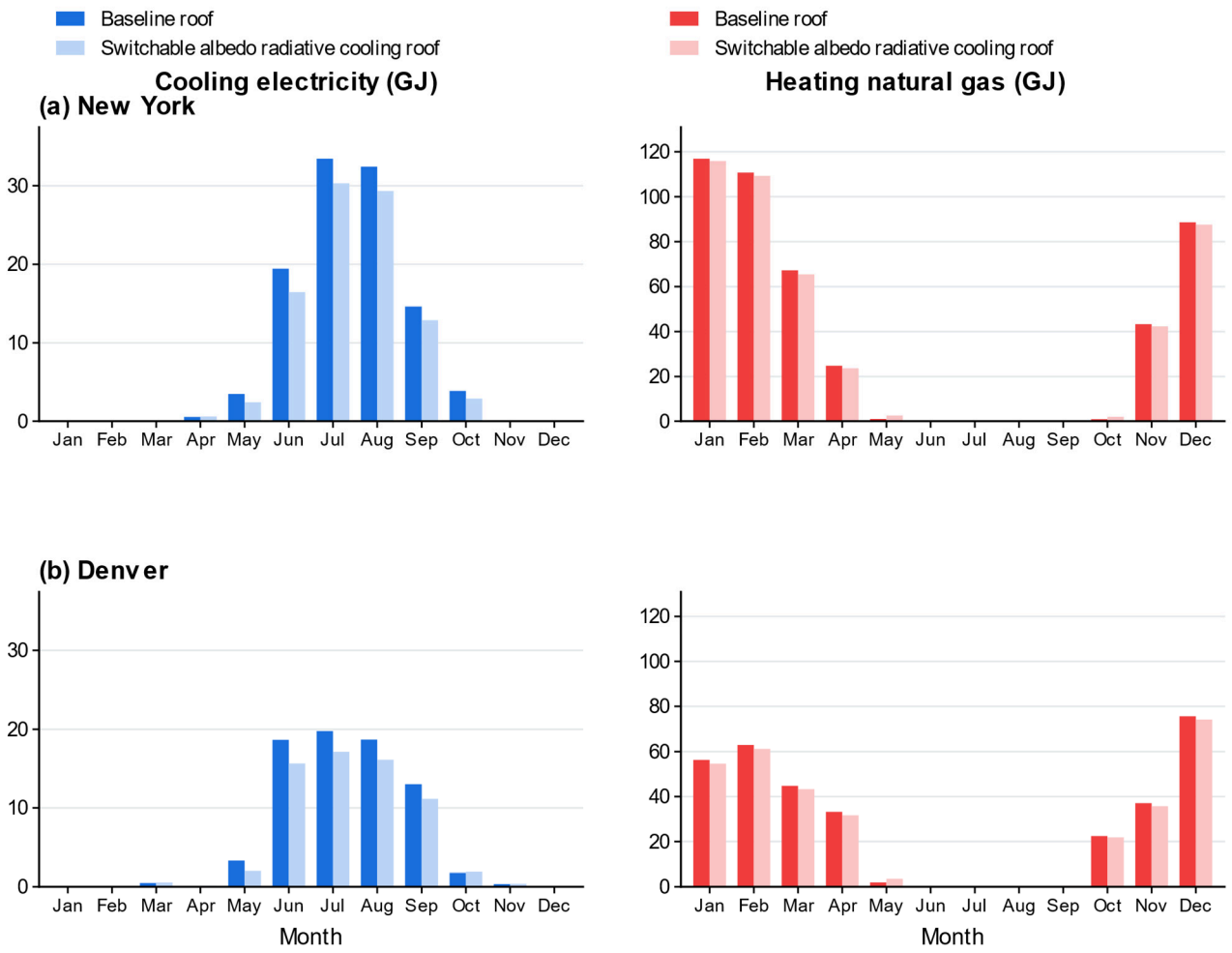


Figure 8. Calculated monthly energy consumption in strip malls with and without the switchable albedo radiative cooling roof in cities in moderate climates: (**a**) New York and (**b**) Denver.

The category of cold climates included Rochester, International Falls, and Fairbanks. In these cities, unlike the situation in the cities in hot climates, the switchable albedo radiative cooling roof was in the heating state in most of the months, which prevented the heating penalty and even saved heating energy, as shown in Figure 9. For example, energy consumption for heating in Rochester was reduced by 4.0% in October. In these cities in cold climates, annual cooling energy use was substantially lower than annual heating energy use.

Figures 7–9 compare monthly cooling electricity and heating natural gas use for the baseline roof and the switchable albedo radiative cooling roof in the eight cities. The number of months assigned to the heating state generally increased from hot to cold climates.

3.3. Comparison Among Different Roofs

Based on the operating state patterns for the switchable albedo radiative cooling roof and the calculated monthly energy consumption, this study further calculated the annual heating and cooling energy consumption for the eight cities. For comparison, these values were also calculated for the non-switchable radiative cooling roof and the traditional cool roof, as shown in Figure 10. For the cities in hot climates, Honolulu, Tucson, and San Diego, the heating energy consumption was negligible. However, for the other cities, the non-switchable radiative cooling roof and the traditional cool roof caused overcooling in the heating seasons, which increased the annual heating energy consumption by an amount ranging from 2.3% and 1.3%, respectively, in Fairbanks to 15.6% and 8.8%, respectively,

in Denver, compared with the baseline case. In contrast, the switchable albedo radiative cooling roof reduced annual heating energy consumption by 0.2% in Rochester to 2.4% in Denver. For the cooling electricity saving, the performance of the switchable albedo radiative cooling roofs and non-switchable radiative cooling roofs was similar, and better than that of the traditional cool roof. As shown in Figure 10a, both roof types reduced the cooling energy consumption, from a 7.3% reduction in Honolulu to 25.5% in San Diego. As a comparison, the traditional cool roof only reduced the cooling energy consumption by 3.1% in Honolulu and 11.0% in San Diego, respectively.

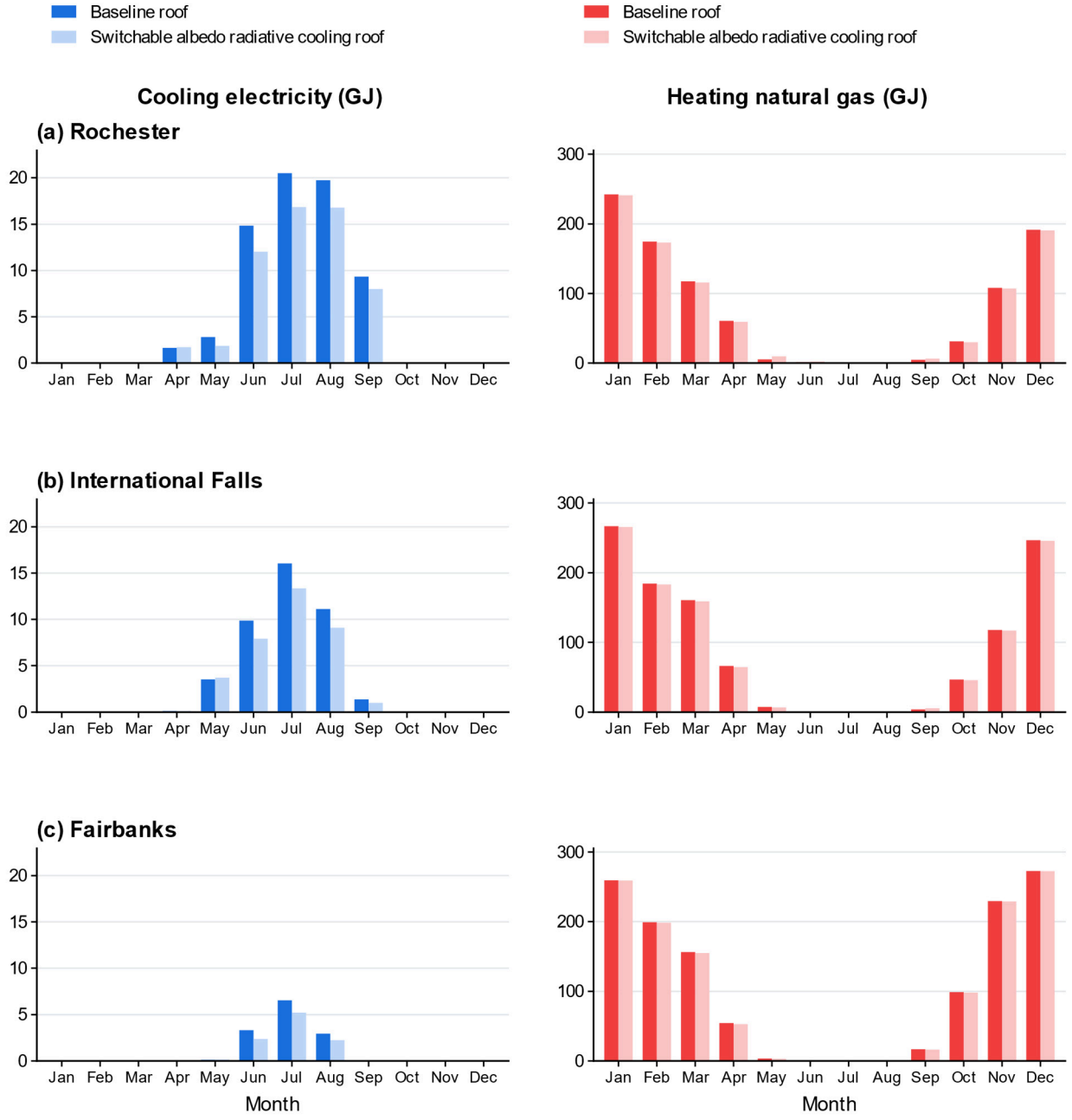


Figure 9. Calculated monthly energy consumption in strip malls with and without the switchable albedo radiative cooling roof in cities in cold climates: (**a**) Rochester, (**b**) International Falls, and (**c**) Fairbanks.

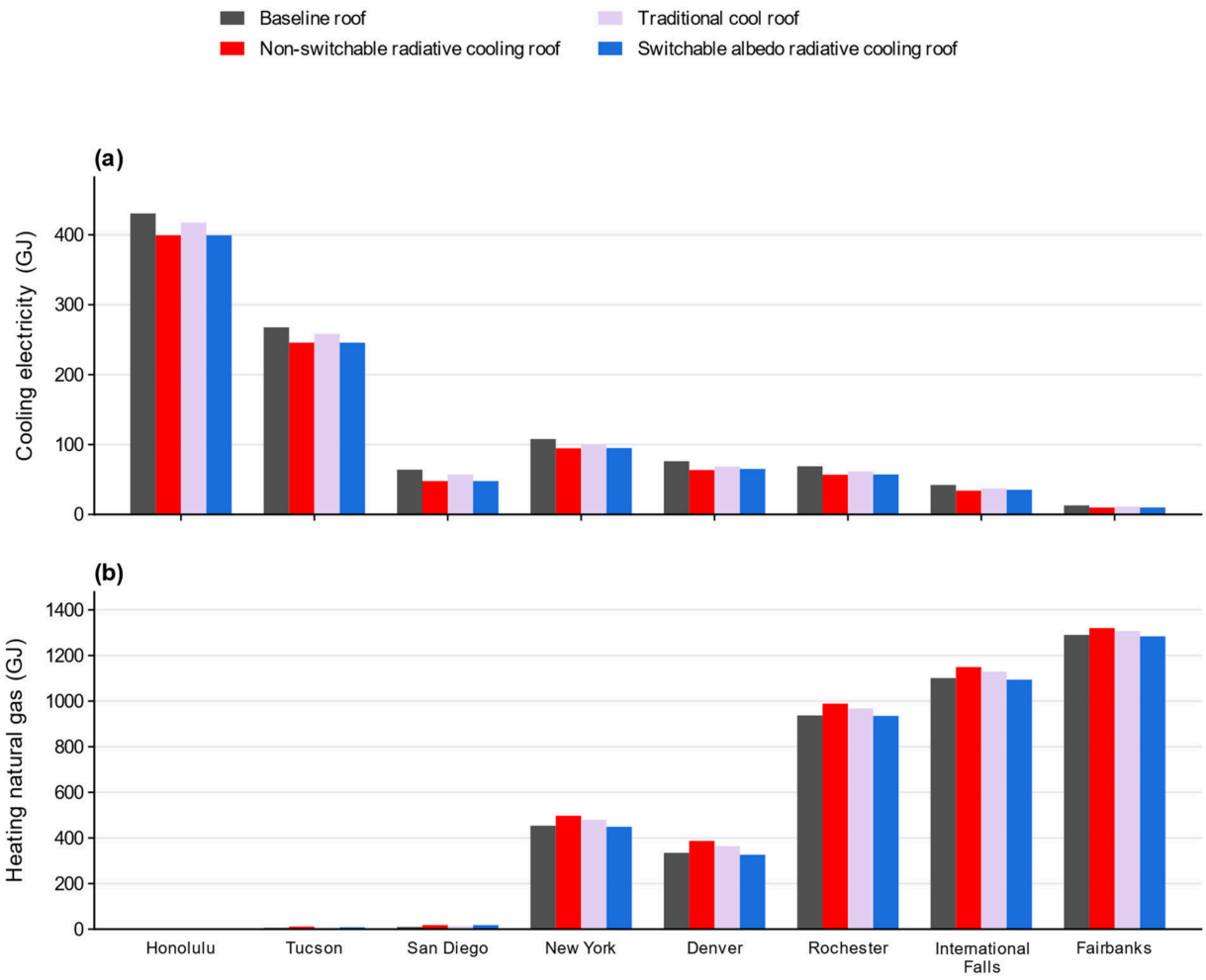


Figure 10. Annual (**a**) cooling and (**b**) heating energy consumption in strip malls with different roofs in the eight cities.

Using the 2018 state-level average retail electricity prices and commercial natural gas prices listed in Table 4, the cooling electricity and heating natural gas consumption shown in Figure 10a,b were converted into the corresponding expenditures. The sum was then regarded as the total cooling and heating expenditure. The net reduction in cooling and heating expenditure when using the cool roofs compared with the baseline can then be calculated. The yearly net reduction in cooling and heating energy expenditures in the strip malls with the use of different roofs in the eight cities is presented in Figure 11. For the switchable albedo radiative cooling roof, annual savings in the hot-climate cities ranged from USD 640 in Tucson to USD 2537 in Honolulu (Table 5). The non-switchable radiative cooling roof showed similar savings in these cities (Figure 11). However, for the cities in moderate climates, using the switchable albedo radiative cooling roof reduced the total expenditure much more than using the non-switchable radiative cooling roof. In New York, the non-switchable radiative cooling roof reduced annual cooling and heating expenditure by 3.2% relative to the baseline roof, whereas the switchable albedo radiative cooling roof achieved a 7.4% reduction. In contrast, the switchable albedo radiative cooling roof reduced annual cooling and heating expenditure by 8.4% relative to the baseline roof. In the cities in cold climates, the use of the non-switchable radiative cooling roof did not reduce the total expenditure and even raised the expenditure by incurring a heating penalty. The switchable albedo radiative cooling roof reduced annual cooling and heating expenditure by 4.2%, 2.8%, and 1.7% in Rochester, International Falls, and Fairbanks, respectively.

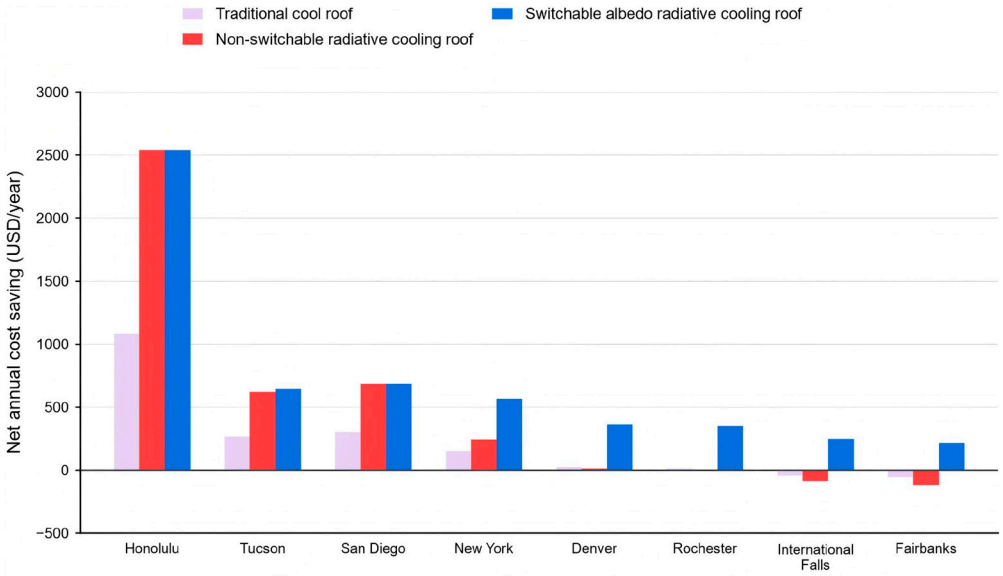


Figure 11. Net yearly reduction in cooling and heating energy expenditure in strip malls with the use of different roofs in the eight cities.

Table 5. Annual cooling and heating expenditure savings achieved by the switchable albedo radiative cooling roof relative to the baseline roof.

Climate	City	Annual Expenditure Saving ($/Year)	Annual Expenditure Saving (%)
Hot	Honolulu	2537	7.3
Hot	Tucson	640	7.9
Hot	San Diego	684	22.6
Moderate	New York	565	7.4
Moderate	Denver	361	8.4
Cold	Rochester	349	4.2
Cold	International Falls	245	2.8
Cold	Fairbanks	216	1.7

Note: Savings were calculated relative to the baseline roof using the 2018 electricity and natural gas prices listed in Table 4. Positive values indicate lower annual cooling and heating expenditure.

Figures 10 and 11 compare the annual energy use and expenditure savings among the roof cases. Table 5 summarizes the annual expenditure saving achieved by the switchable albedo radiative cooling roof relative to the baseline roof in each city, reporting both the absolute value and percentage reduction.

4. Discussion

The results indicate that the primary benefit of the mechanically switchable albedo radiative cooling roof lies in mitigating the seasonal heating penalty of static radiative cooling rather than in further enhancing cooling performance alone. In cities in hot climates, the switchable albedo radiative cooling roofs and non-switchable radiative cooling roofs showed similar cooling energy performance because the high-reflectance cooling state remained favorable for most of the year. In contrast, the benefit of switching became more evident in climates with substantial heating demand. By changing to the low-reflectance state during heating periods, the switchable albedo radiative cooling roof reduced the overcooling penalty while retaining the cooling advantage during warmer periods. The greater annual benefits observed in New York and Denver are consistent with the seasonal balance between cooling and heating demand, but the cross-city comparisons also involve

different prototype roofs. Roof insulation varies across the selected locations (Table 1), while baseline solar reflectance and thermal emissivity differ between the city groups (Table 3). The observed variation therefore reflects the combined influence of climate and prototype properties; this study does not quantify their separate contributions.

The monthly operating state pattern depends on the interaction between climate and building load characteristics. Internal heat gains, envelope insulation, occupancy schedules, and local energy prices can shift the balance between cooling and heating demand. For example, a data center may retain substantial cooling demand even in a cold climate. The monthly operating sequences and associated energy and expenditure savings reported here are specific to the DOE strip mall archetype and the adopted energy price assumptions. The operating state selection procedure could be evaluated for other building types and locations, but their quantitative performance cannot be inferred directly from the present results and would require separate simulations for each building type.

These findings agree with Baniassadi et al. [11], who reported that static super-cool roofs approximately doubled both the cooling energy saving and the heating energy penalty relative to conventional white roofs. In the present study, the non-switchable radiative cooling roof likewise produced greater cooling savings than the traditional cool roof but increased annual heating energy use by 2.3–15.6% in cities with appreciable heating demand. The lower heating penalties than the 11–46% reported in Ref. [11] are likely associated with differences in building archetype, roof insulation, occupancy and HVAC schedules, and climate selection. Studies of roofs with variable reflectance reached a related conclusion. Park and Krarti [34] reported annual energy savings of up to 11% over static cool roofs for commercial buildings, while Testa and Krarti [35] reported additional savings for office buildings of 0.3–3.9%, depending strongly on climate and insulation. Zinzi et al. [36] similarly found that the greatest benefit occurred in climates with substantial cooling and heating demands. Consistent with these studies, the present switchable roof offered little additional benefit over the non-switchable radiative cooling roof in the three cities dominated by cooling demand, whereas annual expenditure savings increased from 3.2% to 7.4% in New York and from 0.3% to 8.4% in Denver. Recent studies of radiative envelopes that adapt to temperature and dynamically integrated radiative cooling and solar heating also identified climate and control strategy as decisive factors [42,43]. No qualitative contradiction was identified, but the reported savings are not directly comparable because the studies considered different building types, climate regions, optical modulation mechanisms, performance metrics, and switching rules. The present study extends this literature by isolating the building energy effect of mechanically switching solar reflectance while maintaining nearly constant longwave emissivity. The adopted monthly operating state strategy provides a consistent basis for comparing different climates, although it does not represent real-time feedback control. Accordingly, the reported savings should be interpreted as the performance achieved under the present monthly switching framework rather than as the maximum potential of the material. At the roof scale, practical implementation of the mechanically switchable coating would require an actuation system capable of applying reversible in-plane deformation while maintaining roof integrity and weather protection. The material could be integrated as a mechanically deformable surface layer, but the actuator configuration, deformation uniformity, structural integration, and maintenance requirements would need to be considered in an actual roofing system. These engineering aspects were not modeled in the present study, which focuses on the building energy implications of the reported optical states. Further studies at the prototype scale are therefore needed to evaluate the feasibility and energy requirements of switching at the roof scale.

Several limitations should be considered when interpreting these results. Mechanical actuation energy was not included in the simulations. Although the selected coating has been demonstrated to switch reversibly through mechanical deformation at the material scale [38], the corresponding study did not define an actuation system at the roof scale or quantify its energy consumption. The reported energy and expenditure savings therefore represent gross benefits at the building level before accounting for the energy required to operate the switching mechanism. At the roof scale, this energy demand would depend on the required stress and strain, the actuated roof area, actuator efficiency, and switching frequency. If the actuation demand is appreciable, the net energy and economic benefits would be lower than the values reported here. Its magnitude cannot be determined until a specific actuator at the roof scale is designed and experimentally characterized. Beyond the energy required for actuation, the predicted performance assumes that the prescribed optical states are fully and uniformly achieved and maintained throughout the service period. In practice, incomplete or nonuniform deformation and actuator downtime could reduce the fraction of the roof operating in the selected state, while cyclic fatigue, creep, aging, weather exposure, and soiling could narrow the effective solar reflectance contrast or modify longwave emittance. Snow coverage could temporarily mask the coating and prevent either optical state from governing the roof surface energy balance. These effects could reduce the realized energy and expenditure savings relative to the idealized simulation results, although their magnitude and climate dependence cannot be quantified without durability at the roof scale and outdoor exposure data. The reported savings should therefore be interpreted as performance under the prescribed optical states rather than as guaranteed field performance.

One limitation is that the monthly roof states were selected using the simulated energy use and expenditure for the complete month. The annual results were then assembled from separate fixed-state simulations, so the procedure does not track the building's transient thermal response following a change in roof state. Switching at a different interval, or using temperature- or load-based control, could change the selected states and estimated annual energy and expenditure savings. These alternatives were not evaluated, so the influence of switching frequency cannot be quantified from the present results.

Mechanical switching also involves physical operations. For the selected coating, changing the optical state requires mechanical stimulation, such as stretching or compression [38]. At the roof scale, the required mechanical action would need to be applied over a large area, and the intended optical state would need to be achieved consistently. If state changes are required daily, repeating these steps reliably across a full roof may be difficult in practice. More frequent switching could also place greater demands on actuator reliability, material durability, and actuation energy. These considerations provide a motivation for investigating less frequent operation but do not demonstrate that daily switching is infeasible or that monthly switching is optimal.

Future work should compare switching intervals through continuous simulations with time-varying roof properties and predefined control rules based on information available at each decision time. Prototype experiments would also be needed to assess practical operation and quantify actuation energy, allowing the net benefits of different switching strategies to be evaluated.

The economic results are also conditional on the adopted 2018 electricity and natural gas prices. Because energy cost was used to select the roof state in months containing both cooling savings and heating penalties, changes in the ratio of electricity to gas prices could alter the selected state in those months with mixed loads and consequently affect the aggregated annual energy use and expenditure. A higher electricity price relative to the natural gas price would place greater weight on cooling electricity savings and would

tend to favor the cooling state. Conversely, a higher natural gas price would increase the economic importance of avoiding heating penalties and would tend to favor the heating state. Although changes in energy prices would not affect the outputs of the individual fixed-state simulations, they could affect the monthly sequence assembled from those simulations. The reported expenditure savings should therefore be interpreted as results under the adopted 2018 price scenario rather than as current or forecast monetary savings.

5. Conclusions

This study evaluated the energy performance of mechanically switchable albedo radiative cooling roofs in strip malls across eight U.S. cities representing different climate conditions. The roof switches between a high-reflectance cooling state and a low-reflectance heating state while maintaining high thermal emissivity. Mechanical actuation energy was not included in the simulations; therefore, the reported savings represent gross energy and expenditure benefits at the building level rather than the net performance of a complete roof system. The analysis also assumes that the prescribed optical states are fully achieved and maintained; incomplete switching or degradation of the optical properties could reduce the benefits realized in practice. The conclusions are also conditional on the prescribed optical properties remaining spatially uniform and time invariant and on the selected state being fully achieved at each scheduled switch. Accordingly, the following conclusions apply to the selected DOE strip mall model under the adopted envelope, HVAC, operating state, optical property, and energy price assumptions:

1. The switchable albedo radiative cooling roof can maintain cooling performance comparable to that of a non-switchable radiative cooling roof while reducing the heating penalty caused by seasonal overcooling. This advantage is mainly achieved by using the high-reflectance state during cooling periods and switching to the low-reflectance state when heating is required.
2. The energy saving benefit of switching varied across the eight city-specific prototype models, which differ in climate, roof insulation, and baseline roof optical properties. In hot climates, the switchable albedo radiative cooling roofs and non-switchable radiative cooling roofs showed similar annual performance because cooling dominated the building load. In moderate and cold climates, the non-switchable radiative cooling roof increased annual heating energy consumption by 2.3–15.6%, whereas the switchable albedo radiative cooling roof avoided this penalty and still provided 12.0–22.8% cooling electricity savings.
3. Under the adopted 2018 electricity and natural gas prices, the estimated economic benefit showed a similar climate dependence. In cities where the non-switchable radiative cooling roof provided limited annual savings or increased heating costs, the switchable configuration reduced annual cooling and heating expenditure by 1.7–8.4% relative to the baseline roof. For these city-specific prototype models, the additional benefit of switching was more evident where both cooling and heating demands were appreciable. The comparisons do not isolate the effect of climate from differences in roof construction and baseline optical properties. The reported savings are estimates under retrospective monthly state selection. Other switching intervals could yield different annual savings, and the present study does not establish an optimal switching frequency.

Author Contributions: Conceptualization, Y.Q. and X.Y.; methodology, Y.Q. and X.Y.; software, Y.Q.; validation, Y.Q. and X.Y.; formal analysis, Y.Q.; investigation, Y.Q.; resources, X.Y.; data curation, Y.Q.; writing—original draft preparation, Y.Q.; writing—review and editing, Y.Q. and X.Y.; visualization,

Y.Q.; supervision, X.Y.; project administration, X.Y.; funding acquisition, X.Y. All authors have read and agreed to the published version of the manuscript.

Funding: This work was supported by the Research Fund of Guangdong Polytechnic Normal University (Grant No. 2026SDKYA113).

Data Availability Statement: The original contributions presented in this study are included in the article. Further inquiries can be directed to the corresponding author.

Acknowledgments: During the preparation of this manuscript, the authors used ChatGPT 6 (OpenAI) for the purposes of polishing language and improving the grammar, clarity, and readability of the text.

Conflicts of Interest: The authors declare no conflicts of interest.

References

1. Testa, J.; Krarti, M. A review of benefits and limitations of static and switchable cool roof systems. *Renew. Sustain. Energy Rev.* **2017**, *77*, 451–460. [CrossRef]
2. Konopacki, S.; Akbari, H.; Pomerantz, M.; Gabersek, S.; Gartland, L.M. *Cooling Energy Savings Potential of Light-Colored Roofs for Residential and Commercial Buildings in 11 US Metropolitan Areas*; Lawrence Berkeley Lab.: Berkeley, CA, USA, 1997. [CrossRef]
3. Hosseini, M.; Akbari, H. Effect of cool roofs on commercial buildings energy use in cold climates. *Energy Build.* **2016**, *114*, 143–155. [CrossRef]
4. Hosseini, M.; Lee, B.; Vakilinia, S. Energy performance of cool roofs under the impact of actual weather data. *Energy Build.* **2017**, *145*, 284–292. [CrossRef]
5. Baniassadi, A.; Sailor, D.J.; Crank, P.J.; Ban-Weiss, G.A. Direct and indirect effects of high-albedo roofs on energy consumption and thermal comfort of residential buildings. *Energy Build.* **2018**, *178*, 71–83. [CrossRef]
6. Shittu, E.; Stojceska, V.; Gratton, P.; Kolokotroni, M. Environmental impact of cool roof paint: Case-study of house retrofit in two hot islands. *Energy Build.* **2020**, *217*, 110007. [CrossRef]
7. Aggarwal, C.; Molleti, S. State-of-the-Art Review: Effects of Using Cool Building Cladding Materials on Roofs. *Buildings* **2024**, *14*, 2257. [CrossRef]
8. Mandal, J.; Yang, Y.; Yu, N.F.; Raman, A.P. Paints as a scalable and effective radiative cooling technology for buildings. *Joule* **2020**, *4*, 1350–1356. [CrossRef]
9. Yu, X.; Chen, C. Mechanisms of enhanced cooling performance of broken hollow microsphere-based radiative cooling coatings. *J. Build. Eng.* **2025**, *113*, 114001. [CrossRef]
10. Mandal, J.; Fu, Y.; Overvig, A.C.; Jia, M.; Sun, K.; Shi, N.N.; Zhou, H.; Xiao, X.; Yu, N.; Yang, Y. Hierarchically porous polymer coatings for highly efficient passive daytime radiative cooling. *Science* **2018**, *362*, 315–319. [CrossRef] [PubMed]
11. Baniassadi, A.; Sailor, D.J.; Ban-Weiss, G.A. Potential energy and climate benefits of super-cool materials as a rooftop strategy. *Urban Clim.* **2019**, *29*, 100495. [CrossRef]
12. Jin, Z.; Zhang, G.; Gong, Q.; Wang, T.; Lu, L.; Dai, J. Enhancing efficient passive daytime radiative cooling in buildings using a durable and robust superamphiphobic coating for long-term performance. *Appl. Energy* **2026**, *413*, 127716. [CrossRef]
13. Lim, X. The super-cool materials that send heat to space. *Nature* **2020**, *577*, 18–20. [CrossRef] [PubMed]
14. Ma, M.; Zhang, K.; Chen, L.; Tang, S. Analysis of the impact of a novel cool roof on cooling performance for a low-rise prefabricated building in China. *Build. Serv. Eng. Res. Technol.* **2021**, *42*, 26–44. [CrossRef]
15. Chen, J.; Lu, L. Comprehensive evaluation of thermal and energy performance of radiative roof cooling in buildings. *J. Build. Eng.* **2021**, *33*, 101631. [CrossRef]
16. Chen, L.; Zhang, K.; Ma, M.; Tang, S.; Li, F.; Niu, X. Sub-ambient radiative cooling and its application in buildings. *Build. Simul.* **2020**, *13*, 1165–1189. [CrossRef]
17. Li, W.; Li, Y.; Shah, K.W. A materials perspective on radiative cooling structures for buildings. *Sol. Energy* **2020**, *207*, 247–269. [CrossRef]
18. Hanif, M.; Mahlia, T.M.I.; Zare, A.; Saksahdan, T.J.; Metselaar, H.S.C. Potential energy savings by radiative cooling system for a building in tropical climate. *Renew. Sustain. Energy Rev.* **2014**, *32*, 642–650. [CrossRef]
19. Lu, X.; Xu, P.; Wang, H.; Yang, T.; Hou, J. Cooling potential and applications prospects of passive radiative cooling in buildings: The current state-of-the-art. *Renew. Sustain. Energy Rev.* **2016**, *65*, 1079–1097. [CrossRef]
20. Panchabikesan, K.; Vellaisamy, K.; Ramalingam, V. Passive cooling potential in buildings under various climatic conditions in India. *Renew. Sustain. Energy Rev.* **2017**, *78*, 1236–1252. [CrossRef]
21. Jeong, S.Y.; Tso, C.Y.; Zouagui, M.; Wong, Y.M.; Chao, C.Y.H. A numerical study of daytime passive radiative coolers for space cooling in buildings. *Build. Simul.* **2018**, *11*, 1011–1028. [CrossRef]

22. Wang, W.; Fernandez, N.; Katipamula, S.; Alvine, K. Performance assessment of a photonic radiative cooling system for office buildings. *Renew. Energy* **2018**, *118*, 265–277. [CrossRef]
23. Yang, R.; Yin, X. Passive cooling in an urban setting. *Nat. Sustain.* **2019**, *2*, 663–664. [CrossRef]
24. Zhao, D.; Aili, A.; Yin, X.; Tan, G.; Yang, R. Roof-integrated radiative air-cooling system to achieve cooler attic for building energy saving. *Energy Build.* **2019**, *203*, 109453. [CrossRef]
25. Zhao, D.; Yin, X.; Xu, J.; Tan, G.; Yang, R. Radiative sky cooling-assisted thermoelectric cooling system for building applications. *Energy* **2020**, *190*, 116322. [CrossRef]
26. Bijarniya, J.P.; Sarkar, J.; Maiti, P. Environmental effect on the performance of passive daytime photonic radiative cooling and building energy-saving potential. *J. Clean. Prod.* **2020**, *274*, 123119. [CrossRef]
27. Yu, X.; Chen, C. A simulation study for comparing the cooling performance of different daytime radiative cooling materials. *Sol. Energy Mater. Sol. Cells* **2020**, *209*, 110459. [CrossRef]
28. Yi, Z.; Lv, Y.; Xu, D.; Xu, J.; Qian, H.; Zhao, D.; Yang, R. Energy saving analysis of a transparent radiative cooling film for buildings with roof glazing. *Energy Built Environ.* **2021**, *2*, 214–222. [CrossRef]
29. Nie, X.; Yoo, Y.; Hewakuruppu, H.; Sullivan, J.; Krishna, A.; Lee, J. Cool white polymer coatings based on glass bubbles for buildings. *Sci. Rep.* **2020**, *10*, 6661. [CrossRef] [PubMed]
30. Chen, J.; Lu, L. Development of radiative cooling and its integration with buildings: A comprehensive review. *Sol. Energy* **2020**, *212*, 125–151. [CrossRef]
31. Zhang, W.; Jiao, D.; Zhao, B.; Pei, G. Experimental and numerical investigation of the effects of passive radiative cooling-based cool roof on building energy consumption. *Appl. Energy* **2024**, *376*, 124161. [CrossRef]
32. Ulpiani, G.; Ranzi, G.; Shah, K.W.; Feng, J.; Santamouris, M. On the energy modulation of daytime radiative coolers: A review on infrared emissivity dynamic switch against overcooling. *Sol. Energy* **2020**, *209*, 278–301. [CrossRef]
33. Li, X.; Sun, B.; Sui, C.; Nandi, A.; Fang, H.; Peng, Y.; Tan, G.; Hsu, P.-C. Integration of daytime radiative cooling and solar heating for year-round energy saving in buildings. *Nat. Commun.* **2020**, *11*, 6101. [CrossRef] [PubMed]
34. Park, B.; Krarti, M. Energy performance analysis of variable reflectivity envelope systems for commercial buildings. *Energy Build.* **2016**, *124*, 88–98. [CrossRef]
35. Testa, J.; Krarti, M. Evaluation of energy savings potential of variable reflective roofing systems for US buildings. *Sustain. Cities Soc.* **2017**, *31*, 62–73. [CrossRef]
36. Zinzi, M.; Agnoli, S.; Ulpiani, G.; Mattoni, B. On the potential of switching cool roofs to optimize the thermal response of residential buildings in the Mediterranean region. *Energy Build.* **2021**, *233*, 110698. [CrossRef]
37. Tian, D.; Zhang, J.; Gao, Z. The advancement of research in cool roof: Super cool roof, temperature-adaptive roof and crucial issues of application in cities. *Energy Build.* **2023**, *291*, 113131. [CrossRef]
38. Zhao, H.; Sun, Q.; Zhou, J.; Deng, X.; Cui, J. Switchable cavitation in silicone coatings for energy-saving cooling and heating. *Adv. Mater.* **2020**, *32*, 2000870. [CrossRef] [PubMed]
39. Li, Y.; Zhang, Z.; Liu, S.; Li, M.; Tso, C.-Y.; Mei, D.; Li, K.; Huang, B. Toward Human Thermal Comfort: An Adaptive Solar-Radiative Thermoregulator. *Adv. Mater.* **2026**, *38*, e21765. [CrossRef] [PubMed]
40. Tang, K.; Dong, K.; Li, J.; Gordon, M.P.; Reichertz, F.G.; Kim, H.; Rho, Y.; Wang, Q.; Lin, C.-Y.; Grigoropoulos, C.P.; et al. Temperature-adaptive radiative coating for all-season household thermal regulation. *Science* **2021**, *374*, 1504–1509. [CrossRef] [PubMed]
41. Sui, C.; Pu, J.; Chen, T.-H.; Liang, J.; Lai, Y.-T.; Rao, Y.; Wu, R.; Han, Y.; Wang, K.; Li, X.; et al. Dynamic electrochromism for all-season radiative thermoregulation. *Nat. Sustain.* **2023**, *6*, 428–437. [CrossRef]
42. Zhang, K.; Zou, Q.; Song, G.; Zhang, Z.; Xiao, F.; Zhang, Y. Energy performance of applying temperature-adaptive radiative envelopes to medium office buildings. *J. Build. Eng.* **2025**, *112*, 113778. [CrossRef]
43. Zhang, W.; Pei, G.; Zhao, B. Performance analysis of switchable radiative cooling and solar heating for building energy-saving. *Energy* **2025**, *333*, 137507. [CrossRef]
44. *ANSI/ASHRAE/IES Standard 90.1-2019*; Energy Standard for Buildings Except Low-Rise Residential Buildings. The American Society of Heating, Refrigerating and Air-Conditioning Engineers: Peachtree Corners, GA, USA, 2019. Available online: https://www.ashrae.org/technical-resources/bookstore/standard-90-1 (accessed on 10 July 2026).
45. U.S. Department of Energy; Building Energy Codes Program; Pacific Northwest National Laboratory. 90.1 Prototype Building Models 90.1-2019—Strip Mall. 2020. Available online: https://www.energycodes.gov/prototype-building-models (accessed on 10 July 2026).
46. Li, T.; Zhai, Y.; He, S.; Gan, W.; Wei, Z.; Heidarinejad, M.; Dalgo, D.; Mi, R.; Zhao, X.; Song, J.; et al. A radiative cooling structural material. *Science* **2019**, *364*, 760–763. [CrossRef] [PubMed]
47. Anand, J.; Sailor, D.J.; Baniassadi, A. The relative role of solar reflectance and thermal emittance for passive daytime radiative cooling technologies applied to rooftops. *Sustain. Cities Soc.* **2021**, *65*, 102612. [CrossRef]

48. *EnergyPlus*; Documentation: Engineering Reference; U.S. Department of Energy: Washington, DC, USA, 2026. Available online: https://energyplus.net/documentation (accessed on 10 July 2026).
49. Yu, X.; Chen, C. Coupling spectral-dependent radiative cooling with building energy simulation. *Build. Environ.* **2021**, *197*, 107841. [CrossRef]
50. Wilcox, S.; Marion, W. *Users Manual for TMY3 Data Sets*; NREL/TP-581-43156; National Renewable Energy Laboratory: Golden, CO, USA, 2008. [CrossRef]
51. U.S. Energy Information Administration (EIA). Sources&Uses. Available online: https://www.eia.gov (accessed on 10 July 2026).
52. Zhao, D.; Aili, A.; Zhai, Y.; Lu, J.; Kidd, D.; Tan, G.; Yin, X.; Yang, R. Subambient cooling of water: Toward real-world applications of daytime radiative cooling. *Joule* **2019**, *3*, 111–123. [CrossRef]

Disclaimer/Publisher's Note: The statements, opinions and data contained in all publications are solely those of the individual author(s) and contributor(s) and not of MDPI and/or the editor(s). MDPI and/or the editor(s) disclaim responsibility for any injury to people or property resulting from any ideas, methods, instructions or products referred to in the content.